

Electrostatic Nonlinear Trimming of Ring-Based MEMS Coriolis Vibrating Gyroscopes

Davin J. Arifin, Stewart McWilliam

Faculty of Engineering, University of Nottingham, UK

Summary. The effects of electrostatic nonlinearity on rate measuring performance of a capacitive MEMS Coriolis Vibrating Gyroscope (CVG) with an imperfect sensing element are investigated. The electrostatic nonlinearity is a result of large amplitude vibration of the ring, which modifies the capacitive forcing and induces self-induced parametric amplification. A cubic-order nonlinear mathematical model is used to describe the electrostatic nonlinearity and expressions are developed for the scale factor and bias. It is shown that parametric pumping induces an amplification range that enhances rate sensitivity and electrostatic non-linearity has potential to negate the effects of imperfection.

Model Description

For MEMS rate-measuring CVG's having a ring resonator [1] the dominant source of nonlinearity is electrostatics due to capacitive actuation and sensing of ring displacements. The dynamics of the sense mode used to detect rate is significantly affected by self-induced parametric amplification [1, 2] when the vibration amplitude is large and the modal properties modulate at twice its vibration frequency. In the small amplitude regime imperfections degrade the scale factor and bias [3]. The potential for nonlinearity to negate or reverse these effects is presented here.

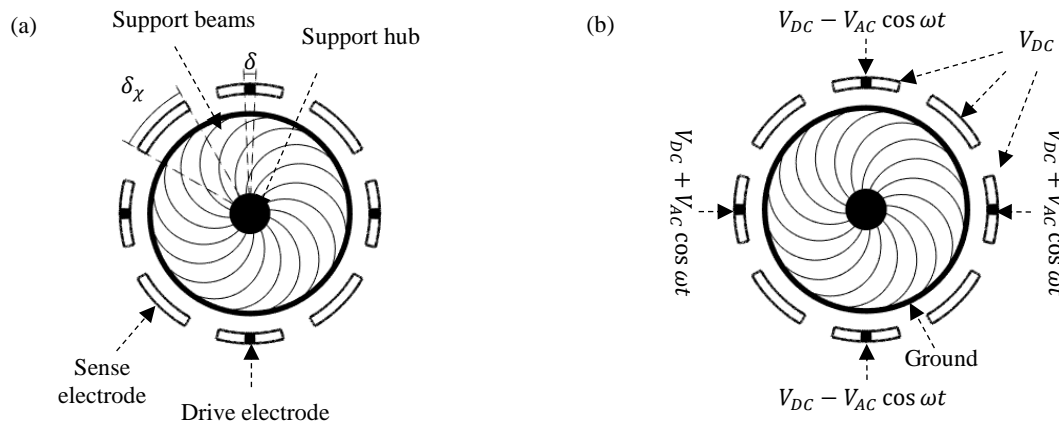


Figure 1: (a) Schematic general layout; (b) voltage profile applied by individual electrodes

Figures 1(a) and 1(b) show the ring element, capacitive electrodes and support structure for a typical device together with the voltages applied across electrode gaps. Voltage V_{AC} drives the ring into its 2θ flexural primary mode. Voltage V_{DC} is primarily responsible for electrostatic nonlinearity. A cubic-order nonlinear model is used to describe the dynamics of the primary (drive) and secondary (sense) modes. Assuming the applied angular rate is much smaller than the natural frequency, $V_{AC} \ll V_{DC}$, and the ring is thin and midsurface-inextensible, the equation of motion for the sense mode is:

$$\ddot{Y} + \frac{\omega_0}{Q} \dot{Y} + Y \left[\omega_0^2 (1 - \mu_\omega \cos 4\theta_\omega) + \kappa \frac{X^2}{g_0^2} \right] = -\frac{8}{5} \dot{X} \Omega - \omega_0^2 \mu_\omega \sin 4\theta_\omega X \quad (1)$$

X, Y are modal coordinates describing the drive and sense modes respectively; ω_0 is the undamped natural frequency and Q is the Q factor for the perfect ring. In practice, $Y \ll X$ so nonlinear terms in Y have been neglected. κ is the nonlinear elastic coupling strength from the drive mode to the sense mode and results in amplitude-dependent resonance. μ_ω is an imperfection parameter and Ω is the applied angular rate. The sense mode is subjected to: i) Coriolis forcing proportional to $\dot{X}\Omega$; ii) imperfection-induced quadrature force proportional to μ_ω ; and iii) parametric excitation arising from nonlinear elastic coupling κ . The drive mode modulates the stiffness of the sense mode at approximately twice its effective vibration frequency. The amplitude and phase of the sense mode oscillation are obtained using the averaging method and the scale factor S^c and bias Ω_0^c are found to be:

$$S^c = -\frac{\frac{8}{5} x \omega_x^2 \left(\frac{\omega_0}{Q}\right)}{\omega_x^2 \left(\frac{\omega_0}{Q}\right)^2 + (\Delta_\omega^2 + \xi_y)(\Delta_\omega^2 - \xi_y)} \quad \Omega_0^c = -\frac{\omega_0^2 \mu_\omega \sin 4\theta_\omega (\Delta_\omega^2 + \xi_y)}{\frac{8}{5} \omega_x^2 \left(\frac{\omega_0}{Q}\right)} \quad (2,3)$$

Here $\Delta_\omega^2 = 2\omega_0^2 \mu_\omega \cos 4\theta_\omega + \frac{x^2}{4g_0^2} (3\gamma - 2\kappa)$ is the frequency detuning parameter and $\xi_y = \kappa \frac{x^2}{4g_0^2}$ is the pumping strength, where γ is the modal Duffing coefficient and x is the drive amplitude. $\kappa, \gamma < 0$ characterize the nonlinear modal stiffnesses and $|\kappa| \leq |\gamma|$, where $|\kappa| = |\gamma|$ when $\delta_\chi = 45^\circ$. For small-amplitude operation, $\xi_y = 0$ and $\Delta_\omega^2 \propto \mu_\omega$.

Nonlinearity causes amplitude-dependent frequency detuning and parametric pumping and both interact with the imperfection to modify the scale factor and bias at large amplitude.

Scale factor and bias

The scale factor for an ideal, linear CVG behaves linearly with drive amplitude x and inversely with bandwidth, so a high Q factor is desirable. In (2) the $(\Delta_\omega^2 + \xi_y)(\Delta_\omega^2 - \xi_y)$ term plays a key role in the nonlinear modification of the scale factor when the amplitude-dependent frequency detuning parameter and parametric pumping strength interact i.e.:

- i. $(\Delta_\omega^2 + \xi_y)(\Delta_\omega^2 - \xi_y) > 0$ - nonlinearity interacts constructively with imperfection, reducing the scale factor.
- ii. $(\Delta_\omega^2 + \xi_y)(\Delta_\omega^2 - \xi_y) = 0$ - nonlinearity negates imperfection effectively trimming the device.
- iii. $(\Delta_\omega^2 + \xi_y)(\Delta_\omega^2 - \xi_y) < 0$ - nonlinear amplification occurs as the effective bandwidth is reduced.

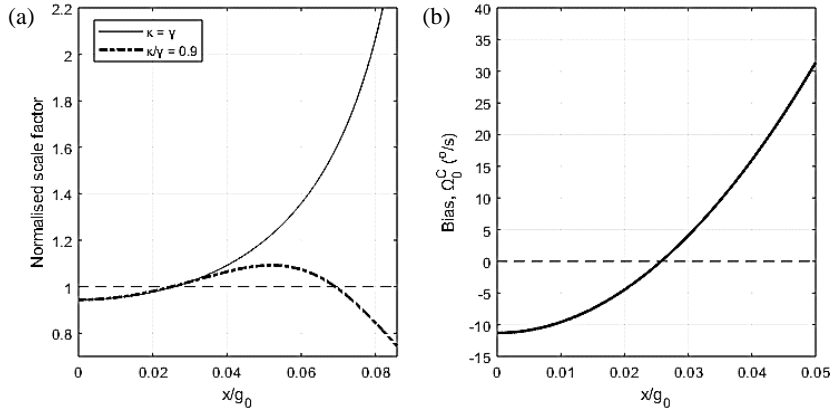


Figure 2: Variation of (a) S^C normalized relative to the trimmed, linear case for continuous ($\kappa = \gamma$) and discontinuous ($|\kappa| < |\gamma|$) biasing electrodes, and (b) Ω_0^C with the gap-normalised drive amplitude

When $(\Delta_\omega^2 + \xi_y)(\Delta_\omega^2 - \xi_y) < 0$ the result is a pure nonlinear effect, because without parametric pumping the imperfection always acts to reduce the scale factor. Figure 2 shows that nonlinear amplification occurs for a range of drive amplitudes. A consequence of this is that the imperfect device has an enhanced scale factor compared to a linear, trimmed device. This amplification range is defined by $-\xi_y < \Delta_\omega^2 < \xi_y$ and the amplification increases as the pumping strength ξ_y increases. The upper bound of this range grows without bound when $\gamma = \kappa$ because the variation of $(\Delta_\omega^2 + \xi_y)(\Delta_\omega^2 - \xi_y)$ with drive amplitude is monotonic in this case, so nonlinear trimming only occurs at the lower bound when the parametric pumping negates the effects of frequency detuning, i.e. $\Delta_\omega^2 = -\xi_y$. In practice higher order nonlinearities play a role in limiting the vibration amplitude. On the other hand, if the difference between γ and κ is large such that $|\kappa| \ll |\gamma|$, which corresponds to the case when the biasing electrode span is small, the upper and lower bounds approach each other and the amplification range reduces. The lower bound of this range when $\Delta_\omega^2 = -\xi_y$ also plays a role in nullifying the bias. Figure 2(b) indicates that the bias is increasingly sensitive to the operational drive amplitude as the amplitude increases. The bias variation is monotonic, either increasing or decreasing, and nonlinear trimming of the device to nullify the bias is only possible if the amplitude dependent frequency detuning is negated by the parametric pumping, i.e. Δ_ω^2 and ξ_y have opposite signs. As electrostatic nonlinearity is softening, this can only occur when the drive excitation is applied at an angular position close to the maximum frequency axis, i.e. $\mu_\omega \cos 4\theta_\omega > 0$.

Conclusions

Electrostatic nonlinearity in ring-based MEMS CVGs interacts with ring imperfections due to self-induced parametric pumping and amplitude-dependent frequency detuning of the modes. These nonlinear effects have potential to negate performance degradation caused by imperfection, effectively trimming the device, but can enhance sensitivity in particular drive amplitude ranges. The lower bound of the amplification range effectively nullifies the bias in the specific case where the frequency detuning is negated by parametric pumping. The performance enhancement offered by electrostatic nonlinearity for imperfect devices is most significant when the cubic-order modal stiffnesses are balanced.

References

- [1] P. M. Polunin and S. W. Shaw, "Self-induced parametric amplification in ring resonating gyroscopes," *International Journal of Non-Linear Mechanics*, vol. 94, pp. 300-308, 2017/09/01/ 2017.
- [2] S. H. Nitzan *et al.*, "Self-induced parametric amplification arising from nonlinear elastic coupling in a micromechanical resonating disk gyroscope," (in eng), *Scientific reports*, vol. 5, p. 9036, Mar 12 2015.
- [3] C. Acar and A. Shkel, *MEMS Vibratory Gyroscopes-Structural Approaches to Improve Robustness*, 1 ed. Springer US, 2009.